Volume 2023, 16 pages | Article ID: IJETS-2310242112864

International Journal of Engineering & Technology Sciences

Journal homepage: http://htpub.org/ IJETS/

ISSN 2289-4152

Analysis of The Impact of Explosive Load on Confined Square Concrete Columns Enveloped with FRP

Hadi Einabadi, Amir Atashi[1]

Department of Civil Engineering, Technical and Vocational University (TVU), Tehran, Iran

Article

Article history:
Received: 21/05/2023
Received in revised form: 10/10/2023
Accepted: 24/10/2023

Keywords:
Concrete Column,
Confinement,
Explosion, FRP sheets,
Square Column,
Finite Element Analysis,
Abaqus

Abstract

In this research, we investigate the behavior of square concrete columns reinforced with FRP (Fiber-Reinforced Polymers) under explosive loading. To achieve this objective, we first reviewed previous studies and selected a reference paper for result validation and simulation in the ABAQUS software. The reinforced concrete column in our study was subjected to an explosive load equivalent to 682 kilograms of TNT at a distance of 6.1 meters. We extracted and compared the displacement at the center of the column with the results presented in the reference paper to validate our simulations. Furthermore, we examined 12 other specimens strengthened with FRP sheets in this research. These 12 specimens were categorized into four groups, each with one parameter variation. In the first category, we varied the thickness of the FRP sheet from 1 to 3 millimeters. In the second category, we altered the orientation of the fibers, using angles of 0, 22.5, and 45 degrees. In the third category, we changed the arrangement of the FRP sheets, including full coverage, one-third on the top and two-thirds on the bottom, and a model with one-third in the middle. Finally, in the fourth category, we varied the column length from 2 to 5 meters, and we investigated how these parameter changes affected the performance of the reinforced column against explosive loads. For the first model with a 1-millimeter thick reinforcing FRP sheet, we obtained a displacement of 35 millimeters. In the second model, where the thickness ranged from one to two millimeters, the center displacement of the column was 28 millimeters. Detailed results for the other models are presented throughout the study.

1. Introduction

Given the increasing frequency of attacks in some regions, there is a growing need to assess and strengthen structures, particularly the columns within each structure, as the heart of a structure, against explosive loads. With advances in science, various methods for strengthening structures and their columns against seismic and explosive loads have been proposed. Zadeh et al. (2023) conducted

[1]Corresponding author at: Technical and Vocational University (TVU), Tehran, Iran.
Email address: hadi.einabadi64@gmail.com

research on one of the strategies employed for reinforcing concrete structures involves the utilization of recycled concrete material. This approach not only promotes sustainability by reducing the demand for virgin concrete but also addresses environmental concerns by repurposing construction waste. Recycled concrete, when appropriately processed and mixed, can exhibit similar structural properties to conventional concrete, making it a viable option for retrofitting projects. By incorporating recycled concrete into retrofitting initiatives, construction professionals can contribute to both cost-effectiveness and eco-friendliness in the construction industry (Zadeh et al., 2023). Among these methods, the strengthening of concrete columns using FRP (Fiber-Reinforced Polymer) sheets has gained significant attention in recent decades. Today, structural strengthening is considered an inevitable and rational measure to ensure the safety of structures. The use of FRP is one of the methods for strengthening reinforced concrete buildings against various external loads. Columns, as the most critical component of structures in providing resistance, stability, and ductility, are of utmost importance. Therefore, the reinforcement of concrete columns using FRP sheets to increase the confinement of concrete and enhance the ductility of structures is widely used in many cases. Due to the importance of flexibility and energy absorption capacity in structures, especially under the influence of explosive loads that involve significant deformations, it is essential for structures and the columns used in them to have good resistance to explosive loads to prevent structural damage. To achieve this goal, methods that increase the ductility of reinforced concrete structures against large deformations are sought. By controlling the lateral expansion of concrete through confinement and restraint, the resistance and ductility of concrete can be significantly increased. One of the most common methods for confining concrete members is using layers and sheets of composite FRP. In this research, an attempt has been made to evaluate the best model and sample of square-reinforced concrete columns with FRP sheets in terms of dimensions, diameter, and thickness of the confining FRP sheets, considering their high resistance to explosive loads. Parameters such as the number of FRP layers, the distance between reinforcing layers, changes in the thickness of FRP sheets, and changes in the amount of reinforcement in the reinforced columns are investigated and analyzed using Abaqus software under explosive loading. The resistance, ductility, and resistance to damage caused by explosions of the samples are compared (Akbarzadeh et al., 2023; Arjomandnia et al., 2023; Khanal et al., 2023; Shabani & Kaviani-Hamedani, 2023; Toosi & Ahmadi, 2023).

The main focus of structural design in the modern era is making sure that structures remain stable under different loads. Some researchers are actively investigating various methods and strategies to improve the reliability of structures under various loads in response to this problem. For instance, in order to better understand the buckling behavior of elliptical CDFST (Concrete-Filled Double-Skin Tube) columns, conducted research in which they added transverse reinforcements to the outer tube. Using Abaqus software, they simulated elliptical columns subjected to compressive force for their study. The investigation's findings show a significant increase in load-bearing capacity, especially for columns with transverse reinforcements, which supports the stability of these columns under load (Mohammed Ali et al., 2024). (Akbari et al., 2013; Nazeryan & Feizbahr) simulated the seismic performance of Composite reinforced concrete and steel (RCS) joints under cyclic and uniform loads using ABAQUS finite element software. A modified model was presented, increasing capacity, and exhibiting more stable behavior, enhancing the system's appeal. Ferdosi and Porbashiri investigated the material properties of carbon nanotubes to use them as a composite to reinforce the structures. They employed the novelty method called the asymptotic homogenization method. Teng and his colleagues first proposed the use of FRP composites for strengthening existing reinforced concrete columns against seismic loads (Teng et al., 2003). Since then, extensive research has been conducted in this field, which will be further examined in the following sections (Hetherington & Smith, 2014). Luccioni and Luege (2006) studied the behavior

of concrete slab elements under explosive loading through experimental tests and numerical modeling, proposing a relationship between the diameter of the explosion-induced cavity, the weight of explosive materials, and the location of the explosion. Shi et al. (2008) conducted research on predicting the damage level of concrete columns under explosive loading by analyzing the pressure-impulse diagram. Sadeghipour and Khorramabadi (2023) examine the behavior of a shape memory alloy brace frame that is buckling constrained under explosive loads. The software ABAQUS was used for the simulation and validation procedures. Sadeghipour (2023) studied explores the explosive behavior of reinforced concrete frames retrofitted with wasp nest dampers, a recent damper type, to understand its effectiveness in reducing structural damage under explosive conditions, despite limited knowledge. (Astarlioglu et al., 2013) examined reinforced concrete columns under combined axial and lateral explosive loads, proposing a one-degree-of-freedom model for analyzing the behavior of reinforced concrete columns under explosive loading. Van Mier et al. (2013) numerically simulated the damage to concrete columns under explosive loading, focusing on the reduction in load-carrying capacity. They identified parameters such as column thickness, radial distance from the explosion, and material properties as critical factors. Li and Hao (2014) conducted a numerical study on the failure of concrete columns under explosive loading, comparing their results with experimental data. They also investigated various parameters, including the distance to the explosion site, column stiffness, and boundary conditions.

2. Research Foundation

In this article, modeling in the Abaqus software will be presented in two sections. In the first section, the fundamentals and methods related to modeling for validation samples will be provided, and after that, the other models of this study will be fully explained.

2.1. Modeling of Validation Sample

All papers In this section, a validation model from the paper Esmailnia (2017) was selected for modeling and simulation in the Abaqus software. The geometry details, material properties, and explosion load used in this column are presented below, and ultimately, the displacement diagram of the column is compared and validated with the displacement diagram presented in the (Esmailnia, 2017). The geometry used in this section is a square column with dimensions of 750*750 millimeters and a length of 3650 millimeters, and its cross-sectional geometry and schematic representation are shown in Figures 1 and 2.

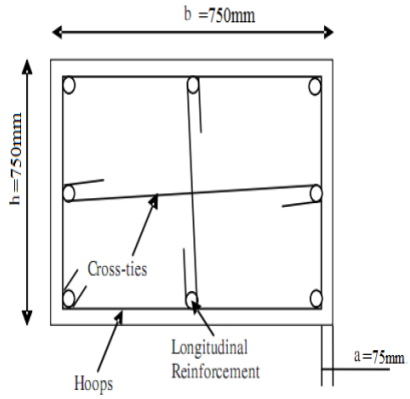

Figure 1. Cross-sectional geometry of the column along with its reinforcements (Esmailnia, 2017).

Longitudinal reinforcements have a cross-sectional area of 32 millimeters, and transverse reinforcements have a cross-sectional area of 10 millimeters. A schematic of the reinforcement used in the validation sample is presented in Figure 3.

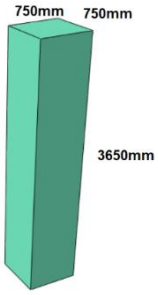

Figure 2. Geometry of the column used in the validation model.

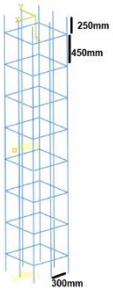

Figure 3. Reinforcement in the validation model.

The materials used in the concrete validation section have a compressive strength of 60 megapascals for concrete and a yield strength of 420 megapascals for steel. Other specifications related to the concrete and steel used in this section are provided in Tables 1 and 2.

Table 1. Concrete Properties in the Validation Model (Esmailnia, 2017).

Density (kilograms per cubic meter)	Elastic Modulus (gigapascals)	Poisson's Ratio	Compressive Strength (megapascals)
2400	29	0.2	34.5

Table 2. Properties Related to Steel Reinforcements in the Validation Model (Esmailnia, 2017).

Ultimate Stress (megapascals)	Yield Stress (megapascals)	Poisson's Ratio	Elastic Modulus (gigapascals)	Density (kilograms per cubic meter)
620	420	0.3	200	7800

To reinforce the concrete and define the rebars in the concrete section, the "Embedded Region" constraint has been used. The lower part of the column is fully constrained, and the explosive load, as shown in Figure 4, is equal to 682 kilograms of TNT and has been applied at a distance of 6.1 meters from the left side of the column.

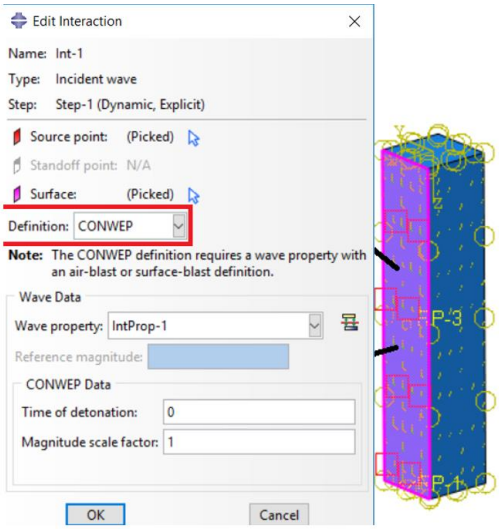

Figure 4. Determination of the Distance and Impact Area of the Explosive Wave in the Validation Model.

The concrete section is meshed using the C3D8R element, which is an 8-node three-dimensional element. The steel reinforcement is meshed using the truss element. A mesh size of 5 centimeters is considered for the concrete, and 1 centimeter is considered for the reinforcement. The meshing of these two sections is shown in Figures 5 and 6.

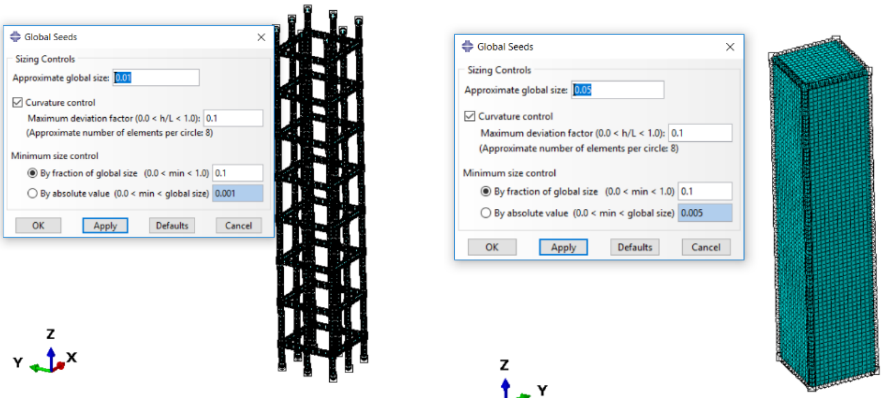

Figure 5. shows the meshing and mesh size for the concrete column and steel reinforcements in the validation model.

3. Models of Research

In this section, the remaining models studied in this research have been simulated in Abaqus software. In this section, an attempt has been made to place FRP sheets with different thicknesses and arrangements on the validation specimen analyzed in the previous section, and the effect of various parameters on each specimen is examined. The analyses have been carried out in four categories.

The first category includes 3 specimens in which the FRP sheet surrounds the concrete column from all four sides. In this category, the effect of FRP sheet thickness on the explosive response of the square concrete column in the validation specimen is investigated. In this category, the first specimen, referred to as M1, has an FRP thickness of 1 millimeter. The second specimen in this category, named M2, has a thickness of 2 millimeters. The third specimen in this category has an FRP thickness of 3 millimeters, and the orientation angle of FRP in all three specimens is zero degrees. A schematic of the FRP used for all three models is presented in Figure 6. FRP in Abaqus is modeled using the Shell property and assigned thickness in the material properties section.

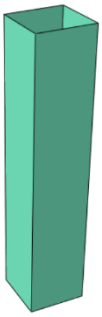

Figure 6. Geometry of the FRP sheets used in the models.

In the second category of this research, three additional models have been considered. In this category, the focus is on examining the orientation angle of FRP fibers with a constant thickness of 2 millimeters and its effect on the explosive response of reinforced square concrete columns. To this end, the first model in this category, referred to as M4, has a zero-degree angle and a thickness of 2

millimeters. The second model in this category, labeled as M5, has a thickness of 2 millimeters and an angle of 22.5 degrees. The third model in this category, named M6, also has a thickness of 2 millimeters but with a 45-degree angle. The other conditions of the problem, such as the amount of explosive material, geometry, and the type of concrete, are similar to the validation model. In the third category of these models, three more samples have been examined, and the parameter under investigation in these three models is the arrangement of FRP sheets. In the first model, labeled as M7, FRP completely surrounds the concrete, with a thickness of 1 millimeter and a zero-degree orientation angle. In the second model in this category, named M8, FRP covers one-third of the upper and one-third of the lower parts of the sample, leaving one-third of the center empty. The thickness and orientation angle are 1 millimeter and zero degrees, respectively. In the third model in this category, labeled as M9, the FRP sheet surrounds one-third of the center while leaving one-third of the upper and one-third of the lower parts empty. Schematics of the FRP sheet used in one-third of the upper and lower parts in model M8 and the schematic of the FRP sheet in one-third of the center are presented in Figure 7.

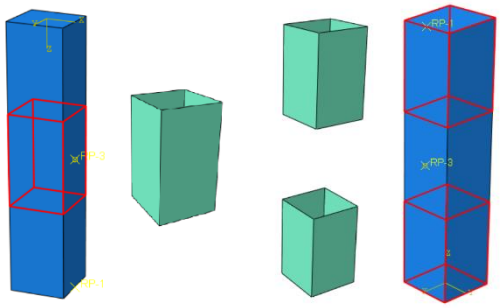

Figure 7. Schematic of the FRP used in one-third of the upper and one-third of the lower parts (right side) and one-third of the center (left side).

In the last category, the effect of column length on its explosive response has also been investigated. In this category, all three samples were wrapped entirely with 1-millimeter thick FRP with a zero-degree orientation angle. The samples had dimensions of 2, 3.65, and 5 meters, respectively, and were named M10, M11, and M12. The material properties used for FRP in this study are presented in Tables 3 and 4. FRP exhibits orthotropic properties and is simulated as a shell in Abaqus software using the Lamina property. The Hashin criterion is used to model the failure of FRP. Additionally, the density of FRP is 1580 kilograms per cubic meter.

Table 3. Properties Used for FRP (Fiber-Reinforced Polymer) (Esmailnia, 2017).

E1 (GPa)	E2(Gpa)	v12	G12(GPa)	G13 (GPa)	G23(GPa)
138	9.65	0.2	5.25	5.25	2.24

Table 4. Failure Properties for FRP According to Hashin Criteria (Esmailnia, 2017).

Maximum Transverse Shear Strength (megapascals)	Maximum Longitudinal Shear Strength (megapascals)	Maximum Transverse Compressive Strength (megapascals)	Maximum Transverse Tensile Strength (megapascals)	Maximum Longitudinal Compressive Strength (megapascals)	Maximum Longitudinal Tensile Strength (megapascals)
71	71	228	57	1440	2280

The other conditions governing the models are consistent with those of the validation model, and in each stage, the FRP sheets are connected to the concrete column using tie constraints. The explosion is applied with an average value of 682 kilograms of TNT from a distance of 6.1 meters in the center of the column. In each sample, the displacement in the center of the column is extracted to compare the effect of parameter changes, and the results are presented comprehensively in the next section.

4. Results

The results presented in this article will be provided similarly to the modeling performed in two sections. In the first section, the results related to the validation model will be presented, and then the results related to the 12 models analyzed in this study will be presented.

4.1. Validation

In this section, the results related to the validation model for explosive loading on the modeled column in the previous section will be presented. The presented results include the displacement in the center of the column, which will be compared with the results presented in this validation model. The comparison of the results obtained from the Abaqus software is shown in Figure 8. The comparison of these analysis results with the reference results (Esmailnia, 2017) is presented in Figure 8.

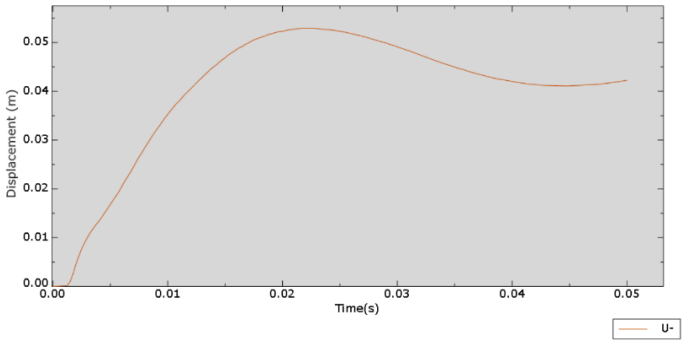

Figure 8. Results Obtained from Abaqus Software for the Validation Model.

As shown in Figure 9, the results obtained from this analysis show very good agreement with the results obtained from the reference (Esmailnia, 2017).

4.2. Results of Other Analyzed Models in this Research

In this section, the results related to the models investigated in this research are presented. These results, as mentioned in Chapter 4, are categorized into four groups, each containing three samples, making a total of 12 samples. The first category examines the effect of FRP thickness on the explosive response of the samples. The second category focuses on the effect of fiber orientation angle on the explosive response of square columns. In the third category, the influence of the arrangement of FRP sheets on the explosive response of square columns will be discussed, and in the fourth category, the impact of column length on its explosive response is investigated. For each category, displacement-time diagrams for the center of the columns are extracted from the Abaqus software and presented for each model. Additionally, contour plots of stress distribution and compressive damage in the columns are also extracted and provided for each column.

4.2.1. Results of Model M1 (Square Column Completely Wrapped with 1mm Thick FRP at 0-Degree Fiber Orientation)

In the initial results presented in this section, the results related to model M1, where FRP completely covered the square column with a thickness of 1mm and had a 0-degree fiber orientation angle, are provided. Displacement-time diagrams for the center of the column, stress distribution, and contour plots of tensile and compressive damage over time for this sample have been extracted and are presented in Figure 10.

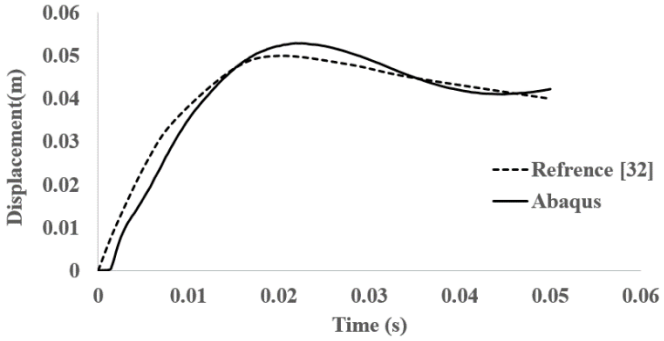

Figure 9. Comparison of Results Obtained for the Validation Model and the Reference Paper (Esmailnia, 2017).

As shown in Figure 10-A, the maximum displacement in the center of the column for this sample is 35 millimeters, and the maximum stress value in sample M1 is 995 megapascals, which occurs on the FRP. By the end of the analysis, the sample is destroyed, as shown in Figures 10-C and 10-D.

4.2.2. Results related to model M2 (Square column completely covered with 2mm thick FRP and 0-degree fiber orientation)

In this section, the results related to model M2 are presented. In the first part, the time-displacement diagram in the center of the column is shown in Figure 11-A, and subsequently, contour plots of stress distribution in concrete, FRP, and contour plots of compressive damage in concrete are presented in Figures 11-B and 11-C, respectively. As resulted in Figure 11-A, the maximum displacement at the center of the column in sample M2 is 28 millimeters, which is a 20% reduction compared to sample M1, where the FRP thickness was 1 millimeter. As shown in Figure 11-B, the highest stress generated in sample M2 is located in the FRP section against the explosion, with a magnitude of 632 megapascals, which is a 30% reduction compared to the stress generated in sample M1, which had a 1-millimeter thickness. According to Figure 11-C, the sample was almost destroyed at the end of the explosion, but the severity of the damage decreased as the thickness of the FRP increased from 1 to 2 millimeters.

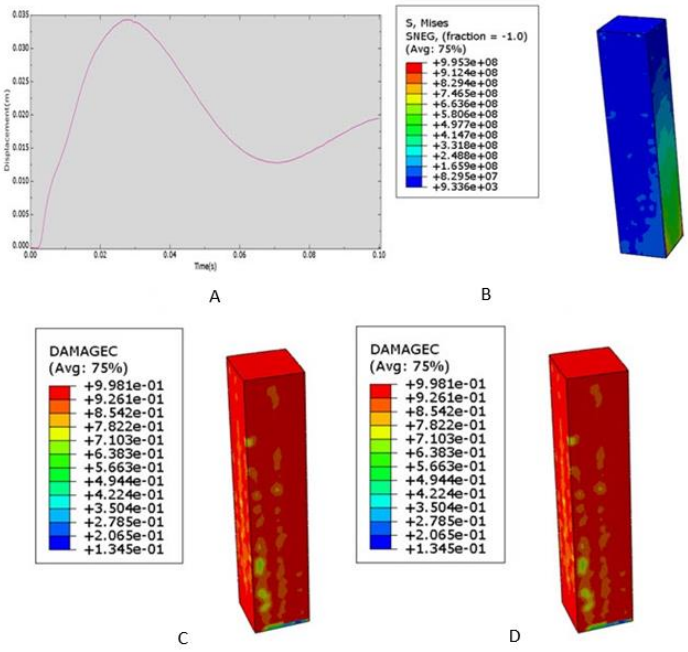

Figure 10. Time-displacement results, stress distribution, and contour plots of tensile and compressive damage for the center of the square column in sample M1. (With complete 1mm thick FRP and 0-degree fiber orientation).

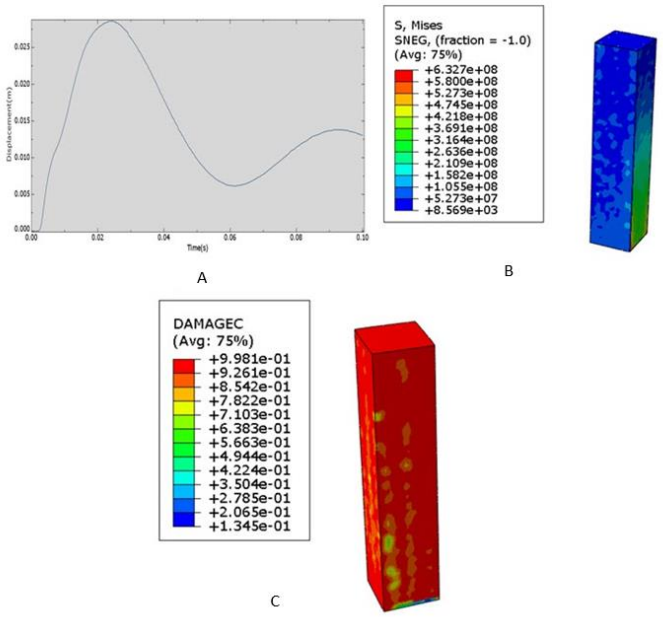

Figure 11. Results of displacement over time for the center of the column, stress distribution, and compressive damage in sample M2. (2-mm thick FRP and 0-degree fiber orientation).

4.2.3. Results for Model M3 (Square Column Fully Wrapped with 3mm Thick FRP and 0-Degree Fiber Orientation)

In this sample, as indicated in the title, the thickness of the FRP has increased to 3 millimeters compared to the two previous samples, while the fiber orientation and other parameters remain unchanged. In Figure 12, the results related to the displacement at the center of the column, stress distribution, and contour of compressive damage are presented.

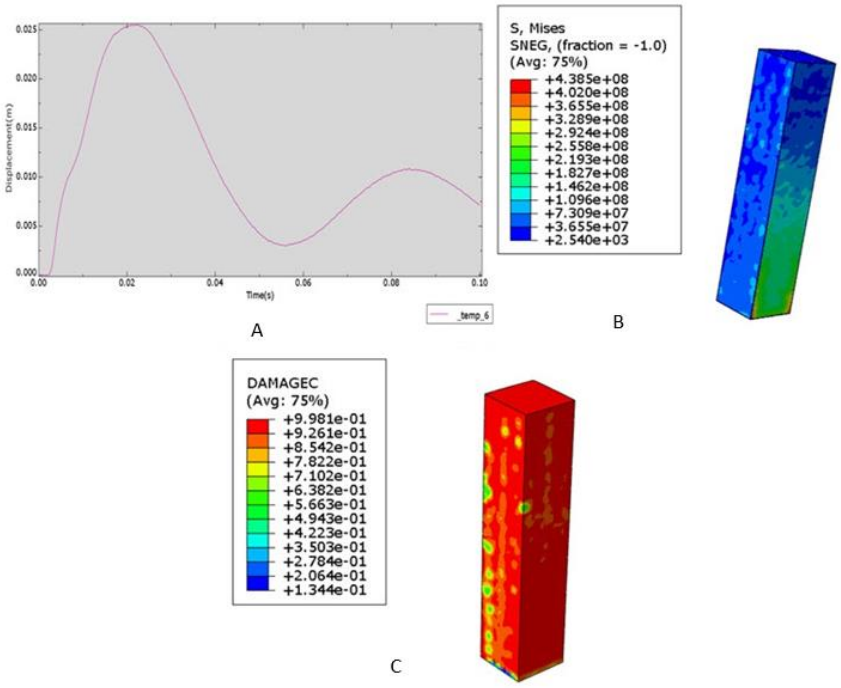

Figure 12. Results of Displacement over Time for the Center of the Column, Stress Distribution, and Contour of Compressive Damage in Sample M3 (Fully Wrapped with 3mm Thick FRP and 0-degree Fiber Orientation).

As shown in Figure 12-A, the maximum displacement in the center of the column in sample M3 is 25 millimeters, which is a 10% decrease compared to sample M2 with a 2-millimeter thickness of FRP and a 29% decrease compared to sample M1 with a 1-millimeter thickness of FRP. Furthermore, as shown in Figure 12-B, the maximum stress in this sample is 438 megapascals (MPa), which is a 24% decrease compared to sample M2 and a 50% decrease compared to sample M1. The intensity of compressive damage in the concrete is also reduced in this sample compared to the two previous samples due to the increased thickness of FRP.

4.2.4. Results for Model M4 (with a thickness of 2 millimeters and a 0-degree orientation)

This sample is exactly the same as sample M2, and its different naming is for classification and comparison purposes within each category. In this sample, the maximum displacement was 28 millimeters, and the maximum stress generated in the sample was 632 megapascals.

4.2.5. Results for Model M5 (with a thickness of 2 millimeters and a 22.5-degree fiber orientation)

In this sample, as mentioned in the previous chapter, the orientation angle of the fibers changed from 0 degrees to 22.5 degrees to investigate the effect of this parameter on the output results. In Figure 13, the results related to the displacement at the center of the column, stress distribution, and pressure damage contours are presented.

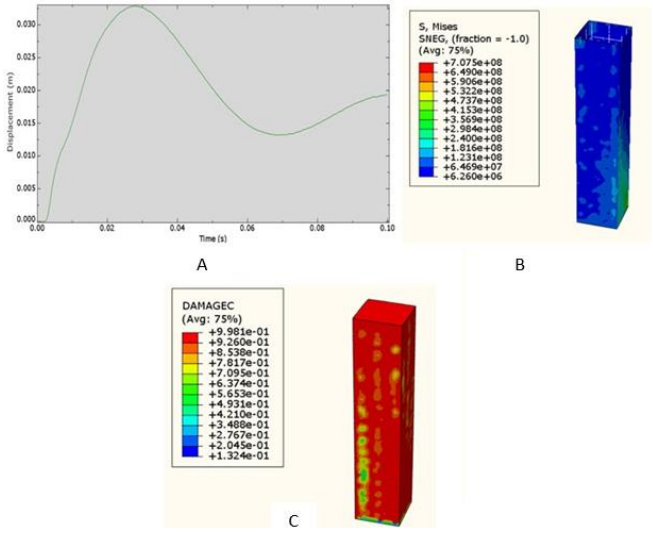

Figure 13. Contours of displacement at the center of the column, stress distribution, and pressure damage in sample M5 (with a thickness of 2 millimeters and a 22.5-degree fiber orientation).

As shown in Figure 13-A, the maximum displacement in the sample with a fiber orientation angle of 22.5 degrees is 33 millimeters, which is an 18% increase compared to sample M4 with a 0-degree angle, where it was 28 millimeters. The reason for this increase is that Young's modulus and tensile strength in the sample are higher in the direction of 1 compared to the direction perpendicular to it, and with an increase in the angle of fiber orientation, the sample becomes weaker. According to Figure 13-B, the maximum stress in the sample is 707 megapascals, which is a 12% increase compared to the previous sample with a 0-degree angle.

4.2.6. Results for Sample M6 (with a thickness of 2 millimeters and 45-degree fiber orientation angle)

In this sample, the fiber angle has changed to 45 degrees. The results related to the maximum displacement in the middle of the column, stress distribution, and pressure damage contours in this sample are presented in Figure 14.

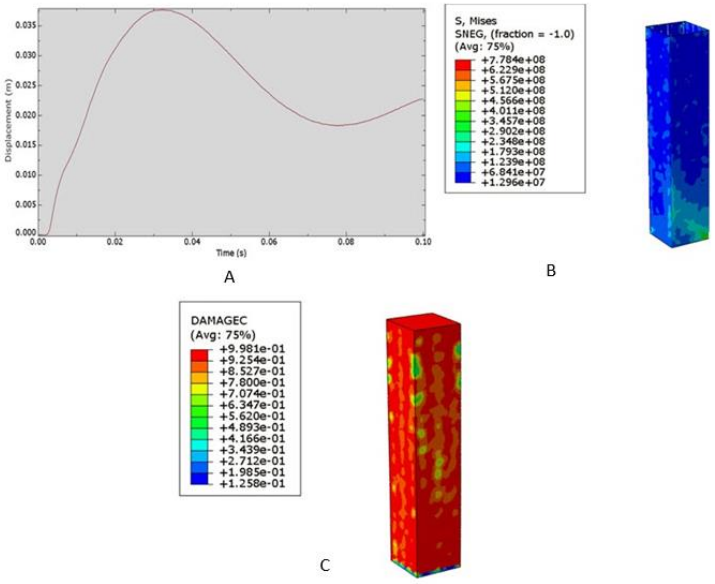

Figure 14. Results of displacement over time for the middle of the column in Sample M6. (With complete 2-millimeter thickness FRP and a fiber orientation angle of 45 degrees).

As discussed in Figure 14-A, the maximum displacement of the column in Sample M6 with a 45-degree fiber orientation angle is 37 millimeters, which has increased by 32% compared to Sample M4 with a 0-degree fiber orientation angle and by 15% compared to Sample M5 with a 22.5-degree fiber orientation angle. As shown in Figure 14-B, the maximum stress in Sample M6 with a 45-degree fiber orientation angle is 778 megapascals, which has increased by 10% compared to Sample M5 with a 22.5-degree angle and by 23% compared to Sample M4 with a 0-degree fiber orientation angle.

4.2.7. Results related to Sample M7 (with a thickness of 1 millimeter and a 0-degree fiber orientation angle, and full FRP)

This sample is the same as Sample M1 and is named differently for categorization and comparison purposes. In this sample, the maximum displacement had a value of 35 millimeters, and the maximum stress created in the sample was 995 megapascals.

4.2.8. Results related to Sample M8 (with a thickness of 1 millimeter, a 0-degree fiber orientation angle, and one-third of the top and bottom covered with FRP)

In this sample, only one-third of the top and one-third of the bottom of the sample are covered with FRP, while one-third in the middle of the sample is concrete without FRP. Subsequently, displacement-time diagrams, stress distribution, and pressure damage contours for this sample are presented in Figure 15.

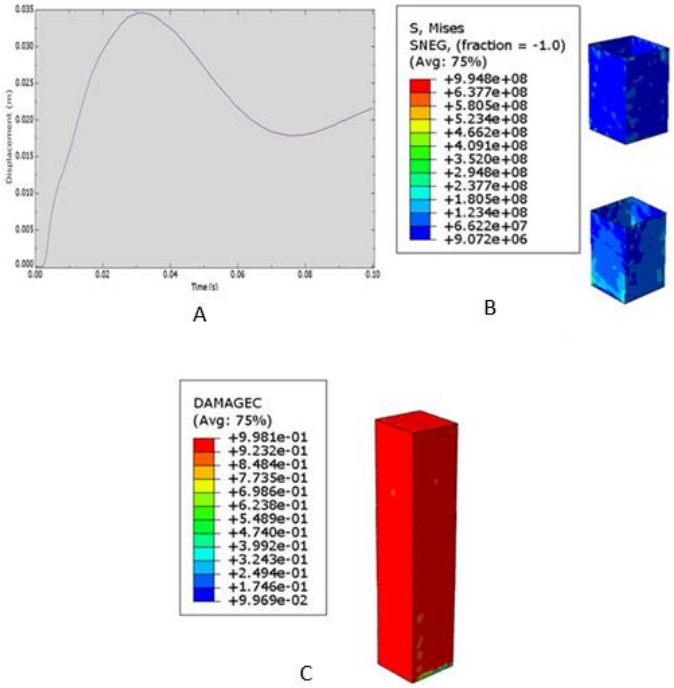

Figure 15. Results of displacement over time for the center of the column, stress distribution, and pressure damage contours in sample M8. (With 1-millimeter thick FRP covering one-third of the top and bottom, and a 0-degree fiber orientation angle).

As shown, the maximum displacement in this sample is equal to sample M7, indicating that by confining the upper and lower parts of the concrete column with FRP sheets, the column behaves very similarly to the fully covered sample. This means that this arrangement can be used instead of full coverage, significantly reducing costs. As observed in Figures 15-A and 15-C, stress contours and pressure damage in the sample also show little difference compared to the fully covered FRP sample, with only a slight increase in pressure damage.

4.2.9. Results related to sample M9 (with a thickness of 1 millimeter and a zero-degree fiber orientation angle in one-third of the middle)

In this sample, one-third of the middle part of the concrete column is covered with FRP, and this FRP has a thickness of 1 millimeter and a zero-degree fiber orientation angle. In Figure 16, the displacement-time diagram for this sample is presented.

As shown in Figure 16-A, the displacement value in the center of the column for this sample is 53 millimeters, which is an increase of 51 percent compared to samples M7 and M8, which were completely covered and had one-third coverage at the top and bottom.

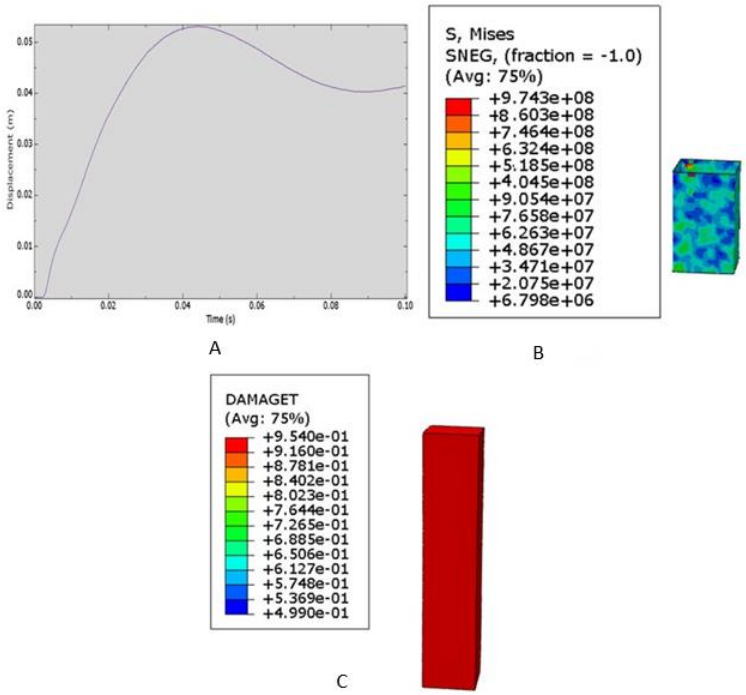

Figure 16. Results of displacement over time, stress distribution, and pressure damage contours for the center of the column in sample M9. (With a 1-millimeter thickness of FRP in one-third of the middle and a zero-degree fiber orientation angle).

As shown in Figures 16-B and 16-C, the stress level in this sample has increased compared to the fully covered sample, and the sample with one-third coverage at the top and bottom. Additionally, the pressure damage has also increased. This indicates that FRP coverage in the middle of the column is not a suitable option for column resistance against explosions.

4.2.10. Results related to sample M10 (with a thickness of 1 millimeter and a 3.65-meter length)

This sample is the same as sample M1 and its different designation is for categorization and comparison purposes. In this sample, the maximum displacement value was 35 millimeters, and the highest stress generated in the sample was 995 megapascals. This group of samples from 10 to 12 examines the effect of the length of the FRP-reinforced column against explosive loads.

4.2.11. Results related to sample M11 (with a thickness of 1 millimeter and a length of 2 meters)

In this sample, the length of the column has been reduced from 3.65 meters to 2 meters. This sample has a complete 1-millimeter thick FRP with a fiber orientation angle equal to zero degrees. Subsequently, the displacement-time graph for this sample is presented in Figure 17.

As shown in Figure 17-A, the displacement in the column has significantly decreased with the reduction in height, going from 35 millimeters in sample M10 with a length of 65.3 meters to 10 millimeters in sample M11 with a length of 2 meters, which represents a 70% reduction. Furthermore, stress and pressure damage contours are provided. As shown in Figure 17-B, the stress in this sample has decreased from 995 to 675 compared to sample M10, resulting in a 32% reduction.

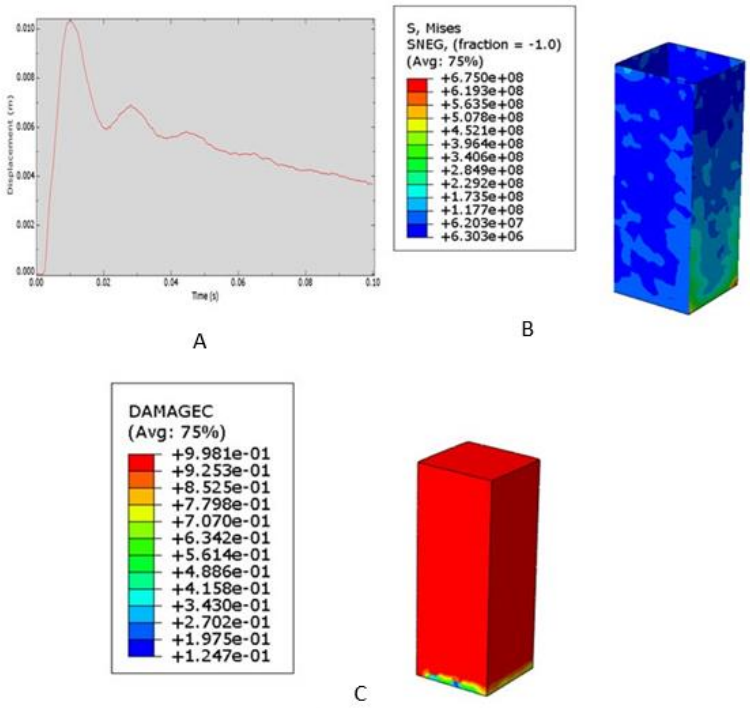

Figure 17. Results of displacement over time, stress distribution, and pressure damage contours in sample M11. (Complete 1-millimeter thick FRP with zero-degree fiber orientation and a length of 2 meters).

4.2.12. Results for Sample M12 (with a thickness of 1 millimeter and fiber orientation angle of zero degrees and a length of 5 meters)

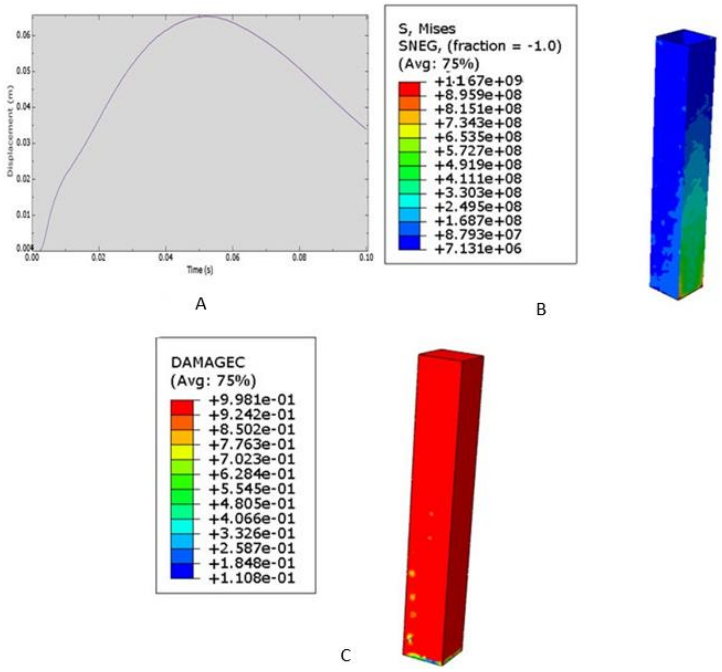

Figure 18. Results of displacement over time for the middle of the column in Sample M12. (Complete FRP with a thickness of 1 millimeter, fiber orientation angle of zero degrees, and a length of 5 meters.)

In this sample, the column's length has increased from 65.3 meters to 5 meters. This sample is equipped with a complete 1-millimeter thick FRP with a fiber orientation angle of zero degrees. The

displacement-time diagram, stress distribution, and pressure damage contours for this sample are presented in Figure 18.

As resulted in Figure 18-A, the displacement value in the column has increased significantly with the increase in height, and its value has increased from 35 millimeters in Sample M10 with a length of 65.3 meters to 65 millimeters in Sample M12 with a length of 5 meters, which represents an increase of 80 percent. According to Figure 18-B, the stress value in this sample has increased from 995 megapascals in Sample M10 with a length of 65.3 meters to 1167 megapascals, indicating a 17 percent increase.

5. Conclusion

In this research, the behavior of square concrete columns reinforced with FRP sheets against explosive loads has been investigated. After reviewing previous research and selecting a reference paper (Esmaeili-Nia and Mahmoudi, 2017), a concrete column with dimensions of 750 by 750 millimeters and a length of 3650 millimeters, reinforced with eight longitudinal rebars with a diameter of 32 millimeters and nine transverse rebars with a diameter of 10 millimeters and spacing of 450 millimeters, was subjected to explosive loading. The modeling process was carried out in the Abaqus software, and the displacement-time curve in the middle of the beam was validated by comparing it with the results of the reference paper.

In the validation model, an explosive load equivalent to 682 kilograms of TNT was detonated at a distance of 6.1 meters from the column. As a result of this explosion, the displacement-time curve in the middle of the beam was extracted and compared with the results of the reference paper (Esmaeili-Nia and Mahmoudi, 2017), showing good agreement between the obtained results.

Continuing this research, 12 concrete column specimens with the specifications of the validation model were retrofitted using FRP sheets, and all 12 specimens were analyzed against an explosive load equivalent to the validation model. In each specimen, the displacement-time curve in the middle of the beam, along with stress and damage contour plots, was extracted. The 12 specimens were classified into 4 groups, and one parameter was varied in each group. The following results were obtained from the conducted analyses in this research:

Increasing the thickness of the FRP sheet significantly reduced the damage inflicted on the concrete column. Increasing the fiber angle resulted in a decrease in the resistance of the FRP sheet.

Partial coverage with FRP sheets (one-third at the top and one-third at the bottom) can be used instead of full coverage, with a similar effect on behavior.

The resistance of the column against explosion increased with a decrease in column length and decreased with an increase in length. These findings provide valuable insights into the behavior of concrete columns retrofitted with FRP sheets against explosive loads, which can inform future design and retrofitting strategies for structures exposed to blast hazards.

References

Akbari, A., Nikookar, M., & Feizbahr, M. (2013). Reviewing Performance of Piled Raft and Pile Group Foundations under the Earthquake Loads. *Research in Civil and Environmental Engineering, 1*(5), 287-299.

Akbarzadeh, M. R., Ghafourian, H., Anvari, A., Pourhanasa, R., & Nehdi, M. L. (2023). Estimating Compressive Strength of Concrete Using Neural Electromagnetic Field Optimization. *Materials, 16*(11), 4200.

Arjomandnia, R., Ilbeigi, M., Kazemidemneh, M., & Hashemi, A. N. (2023). Renovating buildings by modelling energy–CO2 emissions using particle swarm optimization and artificial neural network (case study: Iran). *Indoor and Built Environment*, 1420326X231151244.

Astarlioglu, S., Krauthammer, T., Morency, D., & Tran, T. P. (2013). Behavior of reinforced concrete columns under combined effects of axial and blast-induced transverse loads. *Engineering Structures, 55*, 26-34.

Esmailnia, M. (2017). Reinforcement of reinforced concrete columns under explosive loads using polymer-reinforced fiber coatings. *2*, 55-62.

Ferdosi, S. B., & Porbashiri, M. Calculation of the Single-Walled Carbon Nanotubes' Elastic Modulus by Using the Asymptotic Homogenization Method. *International Journal of Science and Engineering Applications, 11*.

Hetherington, J., & Smith, P. (2014). *Blast and ballistic loading of structures*: Crc Press.

Khanal, M., Zhou, J., & Fan, X. (2023). *Analytical Solution for Moisture Diffusion with Initial Non-Uniform Moisture Concentration used in Bake Time Study in Electronics Packaging.* Paper presented at the 2023 24th International Conference on Thermal, Mechanical and Multi-Physics Simulation and Experiments in Microelectronics and Microsystems (EuroSimE).

Li, J., & Hao, H. (2014). Numerical study of concrete spall damage to blast loads. *International journal of impact engineering, 68*, 41-55.

Luccioni, B. M., & Luege, M. (2006). Concrete pavement slab under blast loads. *International journal of impact engineering, 32*(8), 1248-1266.

Mohammed Ali, A., Besharat Ferdosi, S., Kareem Obeas, L., Khalid Ghalib, A., & Porbashiri, M. (2024). Numerical study of the effect of transverse reinforcement on compressive strength and load-bearing capacity of elliptical CFDST columns. *Journal of Rehabilitation in Civil Engineering, 12*(1).

Nazeryan, M., & Feizbahr, M.(2022) Seismic Evaluation of the Cheng and Chen Modified Model Using Shear Keys in Steel Beam-to-Concrete Column Connections. *Computational Research Progress In Applied Science & Engineering, 8(2), 1-6*

Sadeghipour, A. (2023). Investigation of concrete structures with wasp nest dampers against explosive loads.

Sadeghipour, A., & Khorramabadi, R. (2023). Analyzing the Explosive Behavior of a Buckling Restrained Brace Frame Made of Shape Memory Alloy by Using Finite Element Method. *International Journal of Science and Engineering Applications*.

Shabani, F., & Kaviani-Hamedani, F. (2023). Cyclic response of sandy subsoil layer under traffic-induced principal stress rotations: Application of bidirectional simple shear apparatus. *Soil Dynamics and Earthquake Engineering, 164*, 107573.

Shi, Y., Hao, H., & Li, Z.-X. (2008). Numerical derivation of pressure–impulse diagrams for prediction of RC column damage to blast loads. *International journal of impact engineering, 35*(11), 1213-1227.

Teng, J. G., Chen, J. F., Smith, S. T., & Lam, L. (2003). Behaviour and strength of FRP-strengthened RC structures: a state-of-the-art review. *Proceedings of the institution of civil engineers-structures and buildings, 156*(1), 51-62.

Toosi, G., & Ahmadi, M. M. (2023). *Robust Process Capability Indices for Multivariate Linear Profiles.* Paper presented at the 2023 Systems and Information Engineering Design Symposium (SIEDS).

Van Mier, J., Ruiz, G., Andrade, C., & Yu, R. (2013). Numerical dynamic simulations for the prediction of damage and loss of capacity of RC column subjected to contact detonations.

Zadeh, S. S., Joushideh, N., Bahrami, B., & Niyafard, S. (2023). A review on concrete recycling. *World Journal of Advanced Research and Reviews, 19*(02), 784-793.